Propagation of Bose-Einstein Condensates in a Magnetic Waveguide

A. E. Leanhardt, A. P. Chikkatur, D. Kielpinski, Y. Shin, T. L. Gustavson, W. Ketterle, and D. E. Pritchard *

Department of Physics, MIT-Harvard Center for Ultracold Atoms, and Research Laboratory of Electronics, Massachusetts Institute of Technology, Cambridge, Massachusetts 02139

(Received 9 March 2002; published 2 July 2002)

Gaseous Bose-Einstein condensates of $2-3 \times 10^6$ ^{23}Na atoms were loaded into a microfabricated magnetic trap using optical tweezers. Subsequently, the condensates were released into a magnetic waveguide and propagated 12 mm. Single-mode propagation was observed along homogeneous segments of the waveguide. Inhomogeneities in the guiding potential arose from geometric deformations of the microfabricated wires and caused strong transverse excitations. Such deformations may restrict the waveguide physics that can be explored with propagating condensates. Finer perturbations to the guiding potential fragmented the condensate when it was brought closer to the surface.

DOI: 10.1103/PhysRevLett.89.040401 PACS numbers: 03.75.Fi, 03.75.Be, 39.20.+q

Progress in the field of atom optics depends on developing improved sources of matter waves and advances in their coherent manipulation. Bose-Einstein condensates of dilute alkali vapors [1] are now used as sources of coherent atoms. Miniaturizing the current carrying structures used to confine condensates offers prospects for finer control over the clouds [2,3]. Following the successful trapping and guiding of thermal atoms using self-supported miniature wires [4–8] and substrate-supported microfabricated wire arrays [9–12], recent experiments merged wire traps on the millimeter scale [13] and microfabricated electronic devices [14,15] with Bose-Einstein condensation. This has opened up a front on which further techniques for coherent condensate transport and manipulation can be explored. While condensate guiding with optical potentials may be limited fundamentally by diffraction [16], fundamental limitations to guiding condensates with microfabricated surfaces are not expected for an atom-surface separation in excess of 1 μm [17].

In this Letter, we demonstrate that a Bose-Einstein condensate (BEC) transported with optical tweezers can be transferred into a microtrap on a substrate. Such condensates contained 5 times more atoms than those created in a similar microtrap [14]. We released the BEC from the microfabricated magnetic trap into a single-wire magnetic waveguide and studied its propagation. Condensates were observed to propagate 12 mm before exiting the field of view of our imaging system. We observed single-mode (excitationless) BEC propagation along homogeneous segments of the waveguide in a regime where the longitudinal kinetic energy of the condensate exceeded its transverse confinement energy. Transverse excitations were created in condensates propagating through perturbations in the guiding potential. These perturbations resulted from geometric deformations of the current carrying wires on the substrate. Finer imperfections were observed when trapped condensates were brought closer to the microchip as evidenced by the longitudinal fragmentation of the cloud.

Condensates containing over 10^7 ^{23}Na atoms were created in the $|F, m_F\rangle = |1, -1\rangle$ state in a macroscopic Ioffe-Pritchard magnetic trap [18], loaded into the focus of an optical tweezers beam, and transported over 30 cm in 1250 ms into an auxiliary "science" chamber as described in Ref. [13]. Condensates containing $2-3 \times 10^6$ atoms arrived less than 500 μm below the microfabricated structures mounted in the science chamber. The optical tweezers consisted of 50 mW of 1064 nm laser light focused to a $1/e^2$ radius of 26 μm. This resulted in axial and radial trap frequencies of 4 and 440 Hz, respectively, and a trap depth of 2.7 μK.

A schematic of the microchip onto which the BEC was loaded is shown in Fig. 1. The microfabricated wires lie on a 600 μm thick silicon substrate mounted on an aluminum block. They are 50 μm wide and electroplated with copper to a thickness of 10 μm. The minimum separation distance between wires is 50 μm (100 μm center-to-center). Macroscopic leads that extended to a vacuum feedthrough were attached to the wafer using a gap welding technique. The BEC was initially loaded into a Z-wire trap [9] formed by currents I_1 and I_2 along with an orthogonal magnetic bias field $B_\perp$. Typical loading conditions were $I_1 = I_2 = 1200$ mA and $B_\perp = 5.4$ G, corresponding to a separation of 450 μm between the BEC and the microchip. The longitudinal trap frequency was $\omega_{||} = 2\pi \times 6.0$ Hz and, for a longitudinal bias field $B_{||} = 3.0$ G, the transverse trap frequency was $\omega_\perp = 2\pi \times 97.0$ Hz. Transfer efficiency from the optical tweezers to the Z-wire trap was near unity, and BEC lifetimes over 10 s were observed with the application of a radio frequency (rf) shield [18] which limited the trap depth to ≈ 1 μK and was produced by the current $I_{\rm rf}$ on an auxiliary wire, as shown in Fig. 1.

The BEC was transferred into the waveguide by linearly ramping the current I_2 to zero in 250 ms. The atoms were accelerated into the waveguide by the remaining end cap of the Z-wire trap. Downstream, the effect of this end cap was negligible and we observed BEC propagation at a constant velocity of 3.0 cm/s after a propagation distance of 4 mm for $I_1 = 1200$ mA. Upon releasing the BEC from the Z-wire trap, its longitudinal velocity was controlled by applying an external longitudinal magnetic field gradient

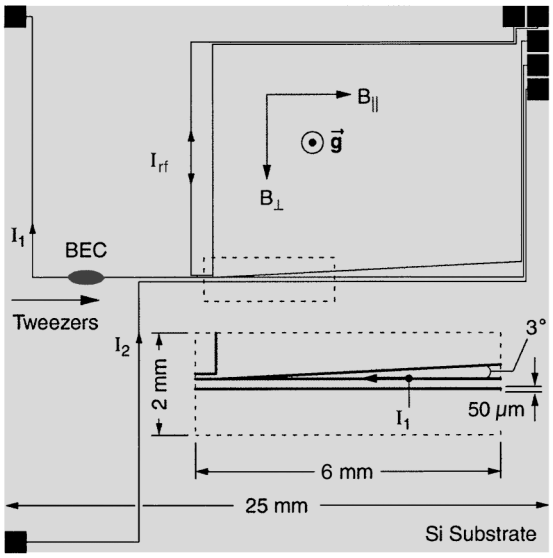

FIG. 1. Microfabricated magnetic trap and waveguide. Optical tweezers loaded a Bose-Einstein condensate into the Z-wire trap formed by currents I_1 and I_2 in conjunction with the magnetic bias field $B_\perp$. Lowering I_2 to zero released the condensate into a single-wire magnetic waveguide. Atom flow was from left to right. The inset shows the widening of the waveguide wire in the region where another wire merges with it at a small angle. The only current flowing in the inset is I_1. The condensate was trapped above the plane of the page and the gravitational acceleration, $\vec{g}$, points out of the page. All microfabricated features are drawn to scale.

created by running current through a single coil coaxial with the waveguide axis. The field gradient was linearly ramped up and down over 6.5 ms to prevent creating excitations and was held constant for 52 ms. With gradients of 0–0.6 G/cm, the atomic velocity was varied over the range 3.0–6.6 cm/s. Throughout this work, condensates were detected via absorption imaging whereby resonant laser light propagating parallel to $B_\perp$ illuminated the atoms and was imaged onto a CCD camera [18].

For all velocities, we observed single-mode condensate propagation along unperturbed sections of the waveguide, as shown in Fig. 3(a) below. The condensate depicted has a smooth shape without any excitations.

Perturbations to the guiding potential arise from geometric deformations of the current carrying wires on the substrate. The extent to which such deformations alter the potential experienced by the atoms depends on the atom-wire separation distance, r, longitudinal extent of the perturbation, ℓ, wire width, w, and wire thickness, t. Under our guiding conditions ($r \gg w, t$) the waveguide potential responds only to changes in the centroid of the current density. In general, only wire deformations with $\ell \gtrsim r$ will significantly perturb the guiding potential due to solid angle considerations. Such a deformation ($\ell \approx 1$ mm, $r = 450$ μm) is depicted in the inset of Fig. 1. As the wire width varies during the bifurcation process, the centroid of the current density will shift in the plane of the microchip. This shift will be mirrored by a shift in the trajectory of the guide in a plane parallel to that of the microchip [19]. Such a shift causes the guide axis to make an angle, θ, with respect to its nominal trajectory along which $B_{||}$ and $B_\perp$ are aligned parallel and perpendicular, respectively. As a result, the effective parallel, $B'_{||}$, and perpendicular, $B'_\perp$, magnetic fields are found by the rotation

$$B'_{||} = B_{||}\cos\theta - B_\perp \sin\theta, \tag{1}$$

$$B'_\perp = B_\perp \cos\theta + B_{||}\sin\theta, \tag{2}$$

where $-\pi/2 \le \theta \le \pi/2$. θ is taken to be a positive (negative) angle for the specific case of atoms entering (exiting) the waveguide perturbation depicted in the inset of Fig. 1.

Since the potential along the waveguide axis is determined by the local magnetic field (due to the Zeeman interaction) and the vertical position of the guide center (due to the gravitational interaction), changes in the effective parallel and perpendicular magnetic fields produce variations in the potential experienced by the propagating atoms. Variations in the effective parallel magnetic field are given by (for small angles)

$$\Delta B'_{||} = -B_\perp \sin\theta\,. \tag{3}$$

Thus, atoms entering (exiting) the perturbed guiding region will encounter a magnetic potential well (barrier). Furthermore, changes in the effective perpendicular magnetic field cause the atom-substrate distance to vary by (for small angles)

$$\Delta r = -r\,\frac{\Delta B'_\perp}{B_\perp} = -r\,\frac{B_{||}}{B_\perp}\,\sin\theta\,. \tag{4}$$

Thus, the guide center entering (exiting) the perturbed guiding region will shift towards (away from) the surface of the microchip, and atoms will encounter a gravitational potential barrier (well). For ^{23}Na atoms in the $|1, -1\rangle$ state, the Zeeman interaction energy is $h \times 700$ Hz/mG and the gravitational interaction energy is $h \times 560$ Hz/μm, where h is Planck's constant.

The effects of the perturbation depicted in the inset of Fig. 1 on BEC propagation were studied by varying the incident velocity of the atoms sent into the region. Condensates traveling below 4.5 cm/s were totally reflected from the perturbation, while clouds at speeds above 5.4 cm/s were entirely transmitted. Figure 2 shows the results for intermediate atomic velocities. The local magnetic field in the perturbed guiding region was measured by driving rf spin-flip transitions that removed atoms from the guide [18]. It was found that upon entering (exiting) the perturbed region the magnetic bottom of the guiding potential decreased (increased) by $h \times (50 \pm 10)$ kHz. The signs of these shifts are consistent with those predicted by Eq. (3). The magnitude of the shift in the Zeeman energy upon exiting the guide is also consistent

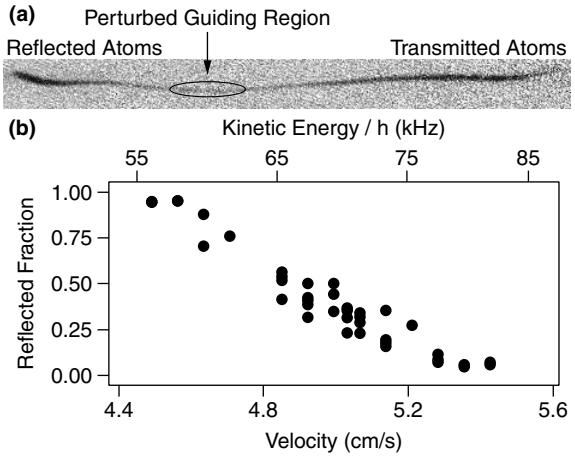

FIG. 2. Bose-Einstein condensates scattering from the waveguide perturbation shown in the inset of Fig. 1. (a) Absorption image after 8 ms of ballistic expansion of a partially transmitted condensate. The incident velocity was 5.0 cm/s. (b) The fraction of atoms reflected as a function of incident velocity. Waveguide parameters for all data were $I_1 = 1200$ mA, $B_\perp = 5.4$ G, $B_{||} = 3.6$ G, and $\omega_\perp = 2\pi \times 84.5$ Hz. The field of view in (a) is 0.35 mm $\times$ 4.00 mm.

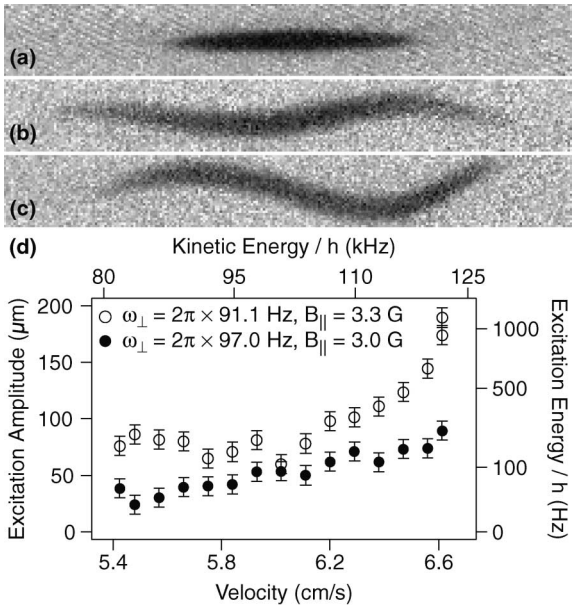

FIG. 3. Bose-Einstein condensate propagation. (a) Absorption image after 10 ms of ballistic expansion of a typical condensate just prior to entering the waveguide perturbation depicted in the inset of Fig. 1. The condensate contained 2×10^6 atoms and was accelerated to a velocity $v = 6.3$ cm/s. It had propagated over 6 mm without excitation in a waveguide with $\omega_\perp = 2\pi \times 84.5$ Hz and $B_{||} = 3.6$ G. Absorption images after 15 ms of ballistic expansion of condensates transmitted through the perturbed guiding region with $v = 6.5$ cm/s for (b) $\omega_\perp = 2\pi \times 97.0$ Hz and $B_{||} = 3.0$ G and (c) $\omega_\perp = 2\pi \times 91.1$ Hz and $B_{||} = 3.3$ G. (d) Peak-to-peak amplitudes of condensate excitations after 15 ms of ballistic expansion versus velocity. For all data $I_1 = 1200$ mA and $B_\perp = 5.4$ G. All transmitted condensates propagated 4 mm beyond the perturbed guiding region before being imaged. The field of view in (a)–(c) is 0.26 mm $\times$ 2.00 mm.

with the onset of transmission through the perturbed guiding region, as shown in Fig. 2(a). From Eq. (3) with $B_\perp = 5.4$ G, the maximum angular deviation, θ_m, of the waveguide trajectory necessary to produce a $h \times 50$ kHz perturbation to the Zeeman energy is $\theta_m = 13$ mrad. The corresponding vertical displacement of the guide center from Eq. (4) with $B_\perp = 5.4$ G, $B_{||} = 3.6$ G, and $\theta_m = 13$ mrad is 4 μm. This yields a gravitational potential variation of $h \times 2.2$ kHz, which is small compared to the Zeeman energy shifts associated with the perturbation.

In the propagation regime where the longitudinal kinetic energy of the BEC is large compared to the transverse confinement energy of the guide, perturbations involving transverse shifts in the guide trajectory are expected to transversely excite incident condensates. Figure 3 depicts such transverse excitations for condensates transmitted through the waveguide perturbation depicted in the inset of Fig. 1. The incident BEC velocity was in the range 5.4–6.6 cm/s. Excitations were characterized by the peak-to-peak amplitude of the transverse displacement of the BEC after ballistic expansion. The imaging axis only provided sensitivity to transverse excitations in the plane normal to the surface of the microchip.

The nearly sinusoidal nature of the BEC excitations shown in Figs. 3(b) and 3(c) indicates that the dipole mode of the BEC was primarily excited. Further evidence for this comes from the fact that little variation in the excitation amplitude as a function of the propagation time after exiting the perturbed guiding region was observed. Conversely, transmitted condensates showed strong signs of higher order excitations when $B_{||}$ was increased beyond 3.6 G corresponding to $\omega_\perp \leq 2\pi \times 84.5$ Hz. The absorption images deviated visibly from a smooth sinusoidal shape. In addition, the measured excitation amplitude depended strongly on propagation time, indicting the phasing and dephasing of several excitation modes.

Figure 3(d) shows a clear increase in the excitation amplitude for increasing velocity at fixed $B_{||}$ and $\omega_\perp$ as well as for increasing $B_{||}$ (decreasing $\omega_\perp$) at fixed velocity. Both trends are consistent with the expectation of increased excitations for an increased ratio of atomic longitudinal kinetic energy to transverse confinement energy. The latter trend is also consistent with the expectation of increased excitations for an increased perturbation size since, from Eq. (4), the vertical displacement of the guide center is proportional to $B_{||}$.

Because the perturbations to the magnetic potential above a single wire are due to its geometric deformations, one expects such perturbations to increase as the trap center is brought closer to the surface of the microchip. We observed longitudinal fragmentation of the BEC as the atoms were brought to within 150 μm of the surface (Fig. 4). At 55 μm from the surface the potential developed axial variations with a characteristic length scale

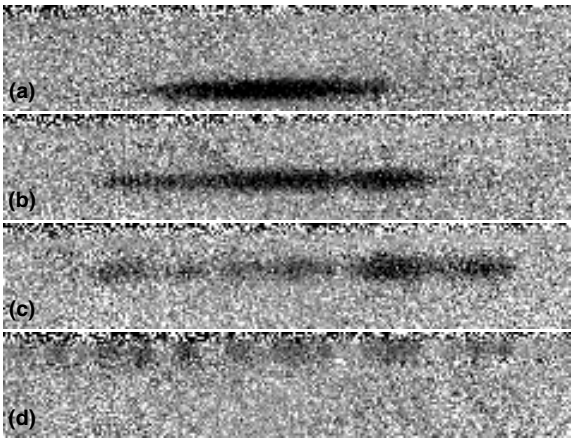

FIG. 4. Fragmented structure of Bose-Einstein condensates brought close to the substrate. Absorption images after 5 ms of ballistic expansion from the Z-wire trap shown in Fig. 1. The atom-substrate separation was (a) 190, (b) 145, (c) 100, and (d) 55 μm. For all images, the condensate started in a trap with $I_1 = I_2 = 540$ mA, $B_\perp = 5.4$ G, and $B_{||} = 0.3$ G corresponding to an atom-substrate separation of 200 μm. The condensate was translated towards the substrate by lowering the wire currents linearly over 500 ms. The atoms were held at their final position for 100 ms prior to trap shutoff. The field of view in (a)–(d) is 0.37 mm $\times$ 2.00 mm.

of 100–150 μm. These variations could be magnetic or gravitational in origin.

In conclusion, we have demonstrated the single-mode propagation of Bose-Einstein condensates in a microfabricated magnetic waveguide and identified sources of transverse excitations. Such excitations need to be addressed to realize the full potential of integrated atom-optical components fabricated on a microchip. In this work, the condensate density was large enough that the mean field energy exceeded the transverse confinement energy. In addition, the longitudinal velocity spread was determined by the mean field expansion of the cloud upon release from the Z-wire trap. The generation of more dilute clouds with narrower longitudinal velocity distributions is possible by continually draining a constant flux of atoms from the Z-wire trap serving as a reservoir. Such a matter wave source is ideal for the realization of an atom interferometer on a microchip.

We are indebted to S. Gupta for contributions to the apparatus, E. Tsikata for experimental assistance, the MIT Microsystems Technology Laboratories for fabricating the microchip used in this work, M. Prentiss and M. Vengalattore for valuable discussions, and A. D. Cronin and D. Schneble for critical readings of the manuscript. This work was funded by ONR, NSF, ARO, NASA, and the David and Lucile Packard Foundation. A. E. L. acknowledges additional support from NSF.

Note added.—Results similar to those in Fig. 4 also appear in Ref. [20]

*http://cua.mit.edu/ketterle_group/

[1] *Bose-Einstein Condensation in Atomic Gases,* Proceedings of the International School of Physics Enrico Fermi, Course CXL edited by M. Inguscio, S. Stringari, and C. E. Wieman (IOS Press, Amsterdam, 1999).

[2] J. D. Weinstein and K. G. Libbrecht, Phys. Rev. A **52**, 4004 (1995).

[3] J. H. Thywissen, M. Olshanii, G. Zabow, M. Drndić, K. S. Johnson, R. M. Westervelt, and M. Prentiss, Eur. Phys. J. D **7**, 361 (1999).

[4] J. Fortagh, A. Grossmann, C. Zimmermann, and T. W. Hänsch, Phys. Rev. Lett. **81**, 5310 (1998).

[5] J. Denschlag, D. Cassettari, and J. Schmiedmayer, Phys. Rev. Lett. **82**, 2014 (1999).

[6] M. Key, I. G. Hughes, W. Rooijakkers, B. E. Sauer, E. A. Hinds, D. J. Richardson, and P. G. Kazansky, Phys. Rev. Lett. **84**, 1371 (2000).

[7] B. K. Teo and G. Raithel, Phys. Rev. A **63**, 031402(R) (2001).

[8] P. Cren, C. F. Roos, A. Aclan, J. Dalibard, and D. Guéry-Odelin, Eur. Phys. J. D (to be published).

[9] J. Reichel, W. Hänsel, and T. W. Hänsch, Phys. Rev. Lett. **83**, 3398 (1999).

[10] D. Müller, D. Z. Anderson, R. J. Grow, P. D. D. Schwindt, and E. A. Cornell, Phys. Rev. Lett. **83**, 5194 (1999).

[11] N. H. Dekker, C. S. Lee, V. Lorent, J. H. Thywissen, S. P. Smith, M. Drndić, R. M. Westervelt, and M. Prentiss, Phys. Rev. Lett. **84**, 1124 (2000).

[12] R. Folman, P. Krüger, D. Cassettari, B. Hessmo, T. Maier, and J. Schmiedmayer, Phys. Rev. Lett. **84**, 4749 (2000).

[13] T. L. Gustavson, A. P. Chikkatur, A. E. Leanhardt, A. Görlitz, S. Gupta, D. E. Pritchard, and W. Ketterle, Phys. Rev. Lett. **88**, 020401 (2002).

[14] H. Ott, J. Fortagh, G. Schlotterbeck, A. Grossmann, and C. Zimmermann, Phys. Rev. Lett. **87**, 230401 (2001).

[15] W. Hänsel, P. Hommelhoff, T. W. Hänsch, and J. Reichel, Nature (London) **413**, 498 (2001).

[16] K. Bongs, S. Burger, S. Dettmer, D. Hellweg, J. Arlt, W. Ertmer, and K. Sengstock, Phys. Rev. A **63**, 031602(R) (2001).

[17] C. Henkel and W. Wilkens, Europhys. Lett. **47**, 414 (1999).

[18] W. Ketterle, D. S. Durfee, and D. M. Stamper-Kurn, in *Bose-Einstein Condensation in Atomic Gases* (Ref. [1]), pp. 67–176.

[19] Analogously, the trajectory will vary in a plane normal to the microchip for variations in the wire thickness.

[20] J. Fortágh, H. Ott, S. Kraft, and C. Zimmermann, cond-mat/0205310.